



TRPV1 activation alleviates cognitive and synaptic plasticity impairments through inhibiting AMPAR endocytosis in APP23/PS45 mouse model of Alzheimer's disease

Yehong Du¹ | Min Fu¹ | Zhilin Huang¹ | Xin Tian² | Junjie Li¹ | Yayan Pang¹ | Weihong Song^{1,3} | Yu Tian Wang^{1,4} | Zhifang Dong¹ 

¹Pediatric Research Institute, Ministry of Education Key Laboratory of Child Development and Disorders, National Clinical Research Center for Child Health and Disorders, China International Science and Technology Cooperation Base of Child Development and Critical Disorders, Chongqing Key Laboratory of Translational Medical Research in Cognitive Development and Learning and Memory Disorders, Children's Hospital of Chongqing Medical University, Chongqing, China

²Department of Neurology, Chongqing Key Laboratory of Neurology, First Affiliated Hospital of Chongqing Medical University, Chongqing, China

³Department of Psychiatry, Townsend Family Laboratories, University of British Columbia, Vancouver, BC, Canada

⁴Brain Research Centre, University of British Columbia, Vancouver, BC, Canada

Correspondence

Zhifang Dong, Pediatric Research Institute, Ministry of Education Key Laboratory of Child Development and Disorders, National Clinical Research Center for Child Health and Disorders, China International Science and Technology Cooperation Base of Child Development and Critical Disorders, Chongqing Key Laboratory of Translational Medical Research in Cognitive Development and Learning and Memory Disorders, Children's Hospital of Chongqing Medical University, Chongqing 400014, China.
Email: zfdong@cqmu.edu.cn

Funding information

National Natural Science Foundation of China, Grant/Award Number: 81571042, 81622015 and 91749116; Innovation Research Group at Institutions of Higher Education in Chongqing, Grant/Award Number: CXQTP19019019034; Natural Science Foundation of Chongqing, Grant/Award Number: cstc2019cyj-bshX0016; Science and Technology Research Program of Chongqing Municipal Education Commission, Grant/Award Number: KJZD-K201900403

Abstract

Alzheimer's disease (AD) is one of the most common causes of neurodegenerative diseases in the elderly. The accumulation of amyloid- β (A β) peptides is one of the pathological hallmarks of AD and leads to the impairments of synaptic plasticity and cognitive function. The transient receptor potential vanilloid 1 (TRPV1), a nonselective cation channel, is involved in synaptic plasticity and memory. However, the role of TRPV1 in AD pathogenesis remains largely elusive. Here, we reported that the expression of TRPV1 was decreased in the brain of APP23/PS45 double transgenic AD model mice. Genetic upregulation of TRPV1 by adeno-associated virus (AAV) inhibited the APP processing and A β deposition in AD model mice. Meanwhile, upregulation of TRPV1 ameliorated the deficits of hippocampal CA1 long-term potentiation (LTP) and spatial learning and memory through inhibiting GluA2-containing α -amino-3-hydroxy-5-methyl-4-isoxazolepropionic acid receptor (AMPA) endocytosis. Furthermore, pharmacological activation of TRPV1 by capsaicin (1 mg/kg, i.p.), an agonist of TRPV1, dramatically reversed the impairments of hippocampal CA1 LTP and spatial learning and memory in AD model mice. Taken together, these results indicate that TRPV1 activation effectively ameliorates cognitive and synaptic functions through inhibiting AMPAR endocytosis in AD model mice and could be a novel molecule for AD treatment.

KEYWORDS

Alzheimer's disease, AMPA receptor endocytosis, capsaicin, learning and memory, long-term potentiation, TRPV1

Du and Fu contributed equally to this work.

This is an open access article under the terms of the Creative Commons Attribution License, which permits use, distribution and reproduction in any medium, provided the original work is properly cited.

© 2020 The Authors. *Aging Cell* published by the Anatomical Society and John Wiley & Sons Ltd.

1 | INTRODUCTION

Alzheimer's disease (AD) is a progressive neurodegenerative disease leading to dementia, which is characterized by extracellular neuritic plaques containing amyloid- β ($A\beta$) peptide deposition and intracellular neurofibrillary tangles consisting of hyperphosphorylated tau protein (Davis & Chisholm, 1999; Goedert et al., 1996). $A\beta$ is derived from sequential proteolytic cleavages of $A\beta$ precursor protein (APP) by β -secretase (BACE1) and γ -secretase (mainly PS1) (Querfurth & LaFerla, 2010). Synaptic plasticity, a cellular basis for learning and memory (Bliss & Collingridge, 1993; Collingridge, Isaac, & Wang, 2004; Malenka & Nicoll, 1999), can be regulated by changing the number, types, or properties of neurotransmitter receptors in post-synaptic densities (Collingridge et al., 2004). Previous studies have well documented that application of $A\beta$ to cultures and slices disrupts spine morphology (Roselli et al., 2005), while in vivo administration of $A\beta$ impairs synaptic plasticity (Shankar et al., 2008) and cognitive function by binding with AMPARs (Hsieh et al., 2006) or N-methyl-D-aspartic acid receptors (NMDARs) (Kamenetz et al., 2003; Snyder et al., 2005) to cause their internalization. These research progresses support the view that $A\beta$ may be the culprit in the synaptic changes during AD development.

The transient receptor potential vanilloid 1 (TRPV1) channel, a ligand-gated nonselective cation channel, can be activated not only by exogenous agonist capsaicin, but also by endogenous compounds such as arachidonic acid metabolites and endocannabinoids (Takahashi & Mori, 2011). TRPV1 is initially thought to be a prominent nociceptive ion channel mainly expressed in afferent sensory neurons (Sawamura, Shirakawa, Nakagawa, Mori, & Kaneko, 2017). However, more and more studies have revealed that TRPV1 is also widely expressed in the brain (Mezey et al., 2000; Toth et al., 2005) and involved in several functions such as the modulation of synaptic transmission and plasticity, as well as cognitive functions (Fu, Xie, & Zuo, 2009). For example, TRPV1 activation by capsaicin enhances NMDAR-dependent CA1 LTP and ameliorates stress-induced memory decline, which can be blocked by TRPV1 antagonists, capsazepine, and SB366791 (Li et al., 2008). Further genetic studies have shown that TRPV1 knockout significantly reduced the LTP in the hippocampus (Hurtado-Zavala et al., 2017; Marsch et al., 2007). Collectively, pharmacological activation of TRPV1 enhances LTP, while the genetic elimination of TRPV1 decreases LTP, suggesting a potential target for TRPV1 in promoting hippocampal LTP, and thus protecting learning and memory (Peters, McDougall, Fawley, Smith, & Andresen, 2010).

Synaptic plasticity and cognitive function are significantly impaired in AD, and we therefore hypothesize that TRPV1 activation may alleviate the impairments of LTP and memory during AD progression. Indeed, our recent study has shown that TRPV1 agonist capsaicin can reverse hippocampal CA1 LTP and memory impairments in the $A\beta$ -induced mouse model of AD (Chen et al., 2017). However, exogenous $A\beta$ treatment is hard to mimic AD development, and so far, little is known about the cellular and molecular mechanism underlying the amelioration of AD symptoms with TRPV1. In the present study, we introduced APP23/PS45 double transgenic model mice

of AD and investigated the influence of TRPV1 on the pathological changes of AD and cognitive functions by using a combination of biochemical, electrophysiological, and behavioral assessments.

2 | RESULTS

2.1 | TRPV1 reduces $A\beta$ generation in APP23/PS45 mice

To examine the effect of TRPV1 on AD development, we first wanted to determine whether there is an alteration of TRPV1 expression in AD. The results showed that the level of TRPV1 protein was significantly reduced in the brain of APP23/PS45 double transgenic AD model mice at the age of 4 months (AD: $40.65 \pm 11.66\%$ relative to WT, $p < .001$ vs. WT; Figure 1a), compared with the age-matched wild-type (WT) littermates. Next, we constructed adeno-associated virus carrying TRPV1 cDNA (AAV_{TRPV1}) or TRPV1 shRNA (AAV_{shTRPV1}) to investigate the role of TRPV1 in the AD pathogenesis. The virus was microinjected into the hippocampus of APP23/PS45 mice to overexpress or knockdown TRPV1. The results showed that the expression of APP (AD + AAV_{EGFP}: $348.68 \pm 38.2\%$ relative to WT, $p < .001$ vs. WT; Figure 1b and d) and its C-terminal fragments (CTFs), including c99 (AD + AAV_{EGFP}: $515.35 \pm 106.14\%$ relative to WT, $p = .005$ vs. WT; Figure 1b and e) and c89 (AD + AAV_{EGFP}: $553.90 \pm 84.31\%$ relative to WT, $p = .009$ vs. WT; Figure 1b and f), were significantly increased in the brain of APP23/PS45 mice compared to WT mice. BACE1 (AD + AAV_{EGFP}: $142.49 \pm 9.37\%$ relative to WT, $p = .001$ vs. WT; Figure 1b and g) and PS1 (AD + AAV_{EGFP}: $150.07 \pm 21.28\%$ relative to WT, $p = .037$ vs. WT; Figure 1b and h) were also significantly increased in APP23/PS45 mice, while upregulation of TRPV1 (AD + AAV_{TRPV1}: $72.98 \pm 7.17\%$ relative to WT, $p = .019$ vs. AD + AAV_{EGFP}; Figure 1b and c) significantly decreased the levels of APP (AD + AAV_{TRPV1}: $249.05 \pm 16.66\%$ relative to WT, $p = .041$ vs. AD + AAV_{EGFP}; Figure 1b and d), c99 (AD + AAV_{TRPV1}: $299.52 \pm 44.78\%$ relative to WT, $p = .021$ vs. WT, $p = .042$ vs. AD + AAV_{EGFP}; Figure 1b and e), BACE1 (AD + AAV_{TRPV1}: $112.86 \pm 10.89\%$ relative to WT, $p = .014$ vs. AD + AAV_{EGFP}; Figure 1b and f), and PS1 (AD + AAV_{TRPV1}: $103.23 \pm 15.26\%$ relative to WT, $p = .049$ vs. AD + AAV_{EGFP}; Figure 1b and f). Notably, downregulation of TRPV1 (AD + AAV_{shTRPV1}: $24.83 \pm 8.91\%$ relative to WT, $p = .025$ vs. AD + AAV_{EGFP}; Figure 1b and c) had no effects on APP (AD + AAV_{shTRPV1}: $366.09 \pm 50.76\%$ relative to WT, $p = .711$ vs. AD + AAV_{EGFP}; Figure 1b and d) and PS1 (AD + AAV_{shTRPV1}: $167.98 \pm 18.52\%$ relative to WT, $p = .437$ vs. AD + AAV_{EGFP}; Figure 1b and h), but significantly increased the expression of c99 (AD + AAV_{shTRPV1}: $759.34 \pm 80.02\%$ relative to WT, $p < .001$ vs. WT, $p = .002$ vs. AD + AAV_{EGFP}; Figure 1b and e) and BACE1 (AD + AAV_{shTRPV1}: $165.25 \pm 4.95\%$ relative to WT, $p = .049$ vs. AD + AAV_{EGFP}; Figure 1b and g). Neither AAV_{TRPV1} nor AAV_{shTRPV1} affected the expression of c89 (AD + AAV_{TRPV1}: $431.13 \pm 50.89\%$ relative to WT, $p = .258$ vs. AD + AAV_{EGFP}; AD + AAV_{shTRPV1}: $835.83 \pm 189.97\%$ relative to WT, $p = .190$ vs. AD + AAV_{EGFP}; Figure 1b and f).

The neuritic plaques formed by $A\beta$ accumulation are a pathological hallmark of AD. Our results have shown that upregulation of TRPV1

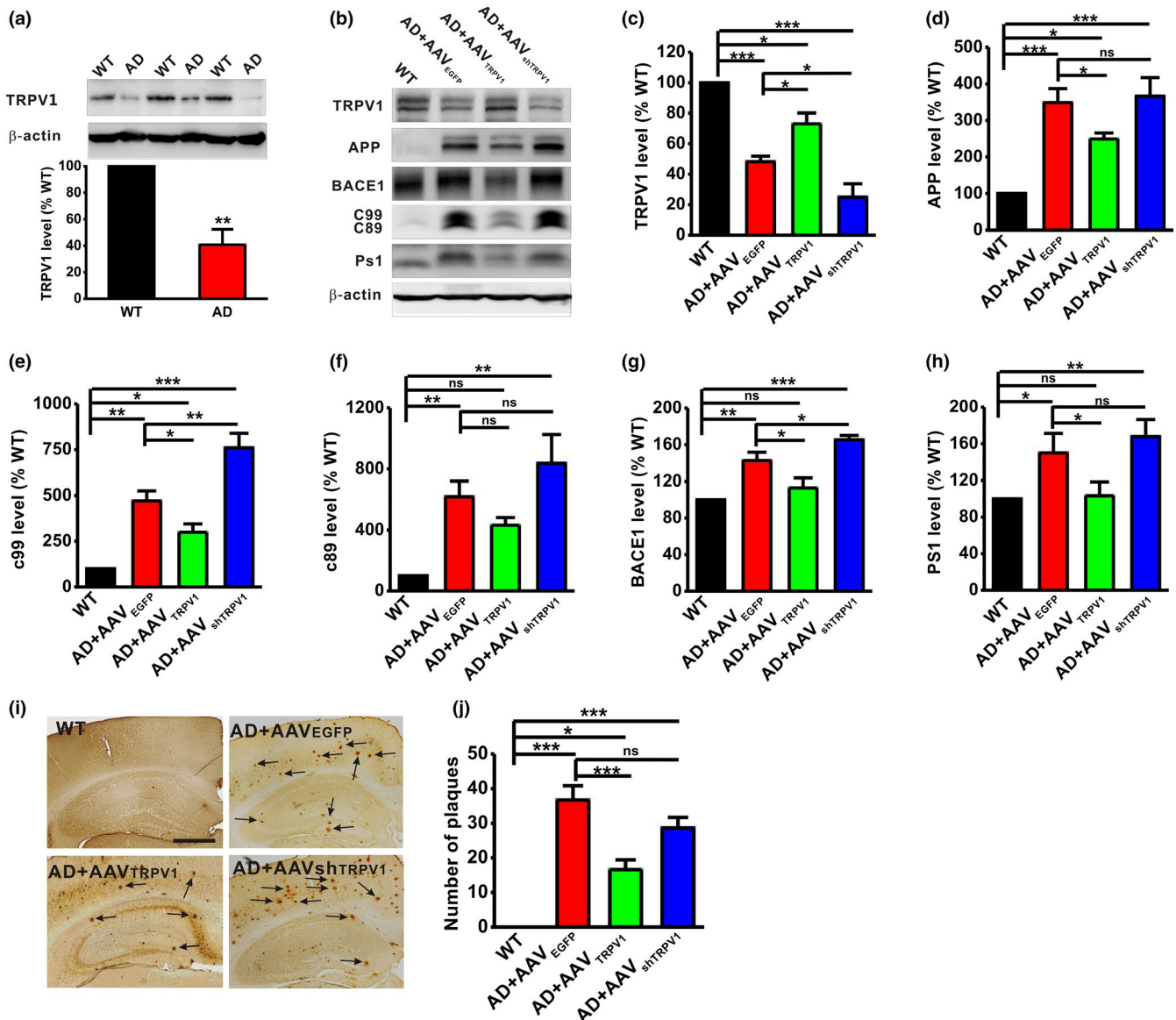


FIGURE 1 TRPV1 decreases APP processing in APP23/PS45 mice. (a) The protein level of TRPV1 in the brains of WT and APP23/PS45 mice at the age of 4 months. $t = 40.605$, $p < .001$ by unpaired Student's t test. $n = 6$ in each group. (b–h) The relative protein levels of TRPV1 (b and c), APP (b and d), c99 (b and e), c89 (b and f), BACE1 (b and g), and PS1 (b and h) are normalized by WT ($n = 4–9$ in each group). One-way ANOVA: $F_{(3,17)} = 28.993$, $p < .001$ for TRPV1; $F_{(3,29)} = 13.818$, $p < .001$ for APP; $F_{(3,13)} = 27.499$, $p < .001$ for c99; $F_{(3,13)} = 7.871$, $p = .004$ for c89; $F_{(3,17)} = 14.975$, $p < .001$ for BACE1; and $F_{(3,25)} = 4.488$, $p = .012$ for PS1. (i and j) The number of neuritic plaques detected by immunohistochemistry in the hippocampus of APP23/PS45 mice ($n = 14–42$ slices from 3–9 mice in each group). One-way ANOVA: $F_{(3,122)} = 15.092$, $p < .001$. Data are expressed as mean \pm SEM, * $p < .05$, ** $p < .01$, *** $p < .001$

alleviates the APP processing. We therefore wanted to determine the effect of TRPV1 on the formation of neuritic plaques in AD model mice. The results showed that upregulation of TRPV1 obviously decreased the number of neuritic plaques in the hippocampus of APP23/PS45 mice (WT: $n = 14$ slices from 3 mice; AD + AAV_{EGFP}: $n = 34$ slices from 8 mice, 36.69 ± 4.13 , $p < .001$ vs. WT; AD + AAV_{TRPV1}: $n = 35$ slices from 9 mice, 16.63 ± 2.78 , $p < .001$ vs. AD + AAV_{EGFP}; Figure 1g and h), whereas downregulation of TRPV1 had no effect on the number of neuritic plaques (AD + AAV_{shTRPV1}: $n = 42$ slices from 9 mice, 28.60 ± 3.11 , $p = .086$ vs. AD + AAV_{EGFP}; Figure 1g and h). These results suggest that TRPV1 downregulates APP processing and A β deposition.

2.2 | TRPV1 rescues hippocampal CA1 LTP in APP23/PS45 mice

Hippocampal LTP has been considered as a cellular mechanism underlying learning and memory (Bliss & Collingridge, 1993; Collingridge et al., 2004; Malenka & Nicoll, 1999). Therefore, we further detected the influence of TRPV1 on hippocampal LTP in AD model mice. Our results showed that a reliable hippocampal CA1 LTP was induced in WT mice (WT: $n = 5$ slices from 5 mice, $165.30 \pm 100\%$ baseline; Figure 2). However, the LTP was apparently impaired in APP23/PS45 mice (AD + AAV_{EGFP}: $n = 5$ slices from 4 mice, $119.71 \pm 3.36\%$

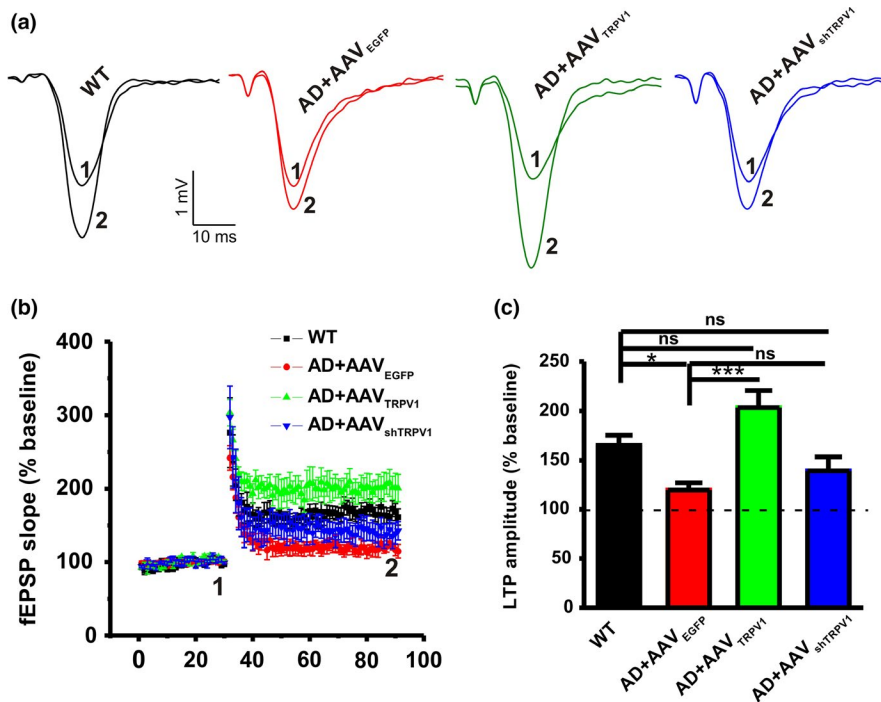


FIGURE 2 TRPV1 rescues the impairment of LTP in the CA1 area of hippocampus in APP23/PS45 mice. Representative fEPSP traces (a) and plots of the normalized slopes (b) of the fEPSP 5 min before and 55 min after TBS delivery. (c) Bar graphs of the average percentage changes in the fEPSP slope 55–60 min after TBS delivery ($n = 5$ –6 slices from 4–6 mice in each group). One-way ANOVA: $F_{(3,19)} = 7.330$, $p = .002$. Data are expressed as means \pm SEM, * $p < .05$, *** $p < .001$

baseline, $p = .036$ vs. WT; Figure 2). Upregulation of TRPV1 could reverse the LTP impairment (AD + AAV_{TRPV1}: $n = 6$ slices from 4 mice, $203.46 \pm 17.22\%$ baseline, $p < .001$ vs. AD + AAV_{EGFP}; Figure 2), whereas AAV_{shTRPV1} treatment had no effect on LTP induction (AD + AAV_{shTRPV1}: $n = 6$ slices from 4 mice, $139.17 \pm 14.29\%$ baseline, $p = .324$ vs. AD + AAV_{EGFP}; Figure 2) in APP23/PS45 mice. Notably, AAV microinjection did not affect basal synaptic transmission because the input-output curve remained unchanged among these groups (Figure S1). Together, these results indicate that TRPV1 could rescue the hippocampal CA1 LTP impairment in AD model mice.

2.3 | TRPV1 inhibits AMPAR endocytosis by interacting with GluA2 subunit

Electrophysiological data have revealed that TRPV1 is able to rescue the hippocampal CA1 LTP in the APP23/PS45 mice, while our recent study has reported that AMPAR endocytosis plays critical role in mediating LTP decay (Dong et al., 2015). In order to detect whether TRPV1 can reverse LTP impairment by affecting AMPAR endocytosis, we next examined the expression of AMPARs including GluA1 and GluA2 subunits in the total lysate and synaptic fraction. The results showed that either upregulation or knockdown of TRPV1 did not affect the expression of total GluA1 (GluA1-TP; Figure 3a) and GluA2 (GluA2-TP; Figure 3b). However, the synaptic protein level of GluA2 (GluA2-SP) was significantly decreased in APP23/PS45 mice (AD + AAV_{EGFP}: $88.02 \pm 1.46\%$ relative to WT, $p = .043$ vs. WT; Figure 3d) compared to the WT group. More importantly, upregulation of TRPV1 restored the expression of synaptic GluA2 (AD + AAV_{TRPV1}: $104.10 \pm 4.60\%$ relative to WT,

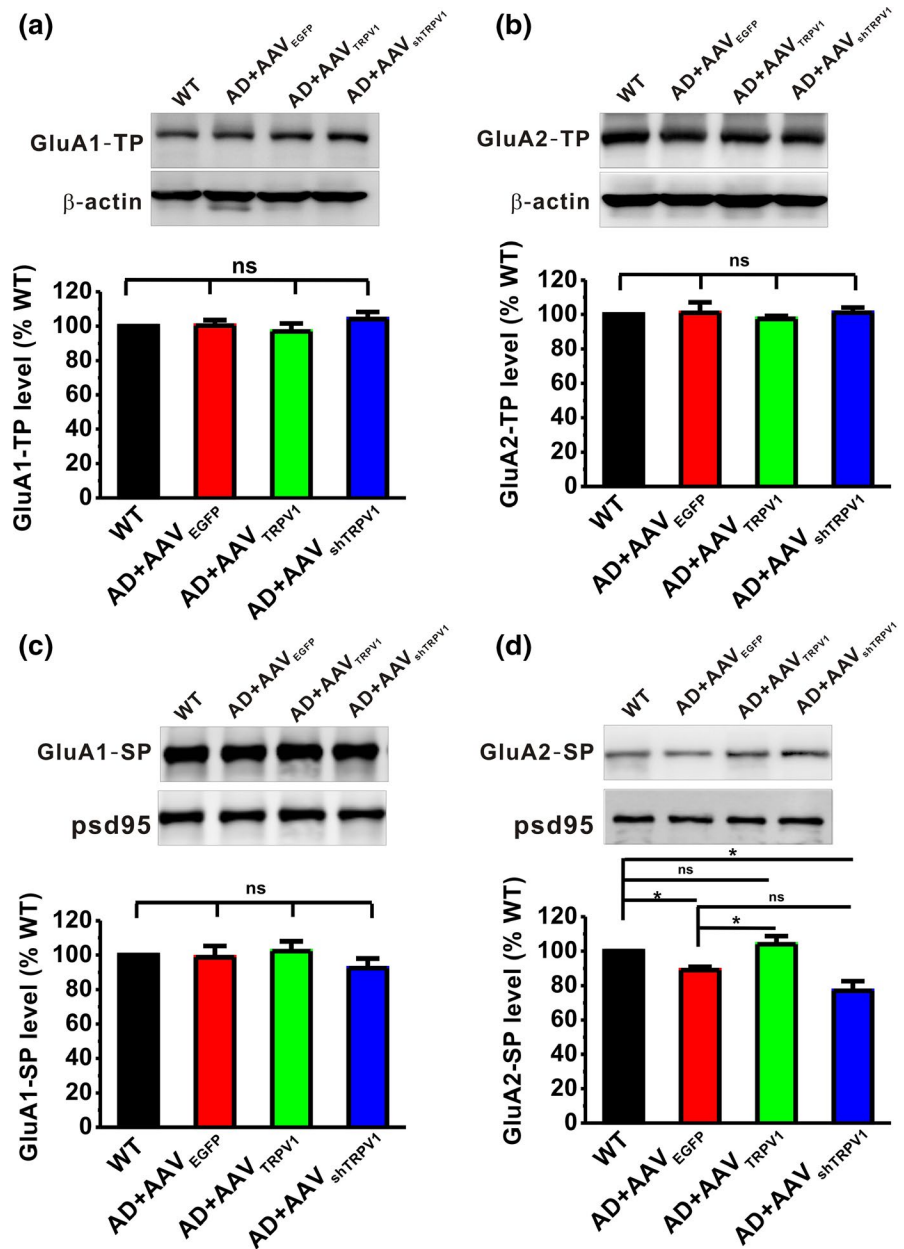
$p = .453$ vs. WT, $p = .010$ vs. AD + AAV_{EGFP}; Figure 3d), whereas AAV_{shTRPV1} had no effect on the synaptic GluA2 expression (AD + AAV_{shTRPV1}: $76.89 \pm 5.72\%$ relative to WT, $p = .001$ vs. WT, $p = .057$ vs. AD + AAV_{EGFP}; Figure 3d). Notably, there was no significant difference in the expression level of synaptic GluA1 among these four groups (Figure 3c).

To determine whether TRPV1 physically associates with AMPARs, and subsequently resulting in AMPAR endocytosis, we next performed co-immunoprecipitation experiments in extracts of brain samples from WT and APP23/PS45 mice. The results demonstrated that TRPV1 co-immunoprecipitated with GluA2 (Figure 4b), but not GluA1 (Figure 4a). To further confirm the finding that TRPV1 only interacted with GluA2, we next used antibodies to GluA1 and GluA2 to precipitate TRPV1 and got the similar results that only GluA2 (Figure 4d), but not GluA1 (Figure 4c), was able to co-immunoprecipitate with TRPV1. More importantly, the interaction of TRPV1 with GluA2 was reduced in APP23/PS45 mice compared to WT, and upregulation of TRPV1 increased the interaction between GluA2 and TRPV1 (Figure 4d). Collectively, these data suggest that expression of TRPV1 regulates AMPAR endocytosis through interaction with the GluA2 subunit.

2.4 | Genetic upregulation of TRPV1 rescues memory decline in APP23/PS45 mice

Aforementioned results have revealed that TRPV1 can reduce AD-related neuropathologies in APP23/PS45 mice. To directly examine whether TRPV1 could alleviate cognitive impairments in these AD model mice, the Morris water maze test was introduced to measure the spatial learning and memory. During the Morris water maze

FIGURE 3 TRPV1 increases the expression of GluA2 in the synapse. The relative protein levels of total GluA1 (a), total GluA2 (b), synaptic GluA1(c), and synaptic GluA2 (d) are normalized by WT mice ($n = 4-6$ in each group). One-way ANOVA: $F_{(3,21)} = 0.707, p = .559$ for total GluA1; $F_{(3,13)} = 0.351, p = .789$ for total GluA2; $F_{(3,21)} = 0.636, p = .601$ for synaptic GluA1; and $F_{(3,13)} = 10.829, p = .001$ for synaptic GluA2. Data are expressed as mean \pm SEM, * $p < .05$



training, the escape latency in APP23/PS45 group (AD + AAV_{EGFP}, $n = 18$) was much longer than those in the WT group (WT, $n = 16$) (Day 1: 77.72 \pm 6.14 s for WT, 89.17 \pm 4.98 s for AD + AAV_{EGFP}; Day 2: 45.66 \pm 6.36 s for WT, 63.48 \pm 6.48 s for AD + AAV_{EGFP}; Day 3: 31.59 \pm 4.35 s for WT, 67.86 \pm 8.97 s for AD + AAV_{EGFP}; Day 4: 24.41 \pm 3.17 s for WT, 59.78 \pm 8.44 s for AD + AAV_{EGFP}; Day 5: 25.94 \pm 2.89 s for WT, 63.41 \pm 9.02 s for AD + AAV_{EGFP}; $p < .001$ vs. WT; Figure 5a). AAV_{TRPV1} (AD + AAV_{TRPV1}, $n = 19$) treatment significantly shortened the escape latency (Day 1: 84.36 \pm 4.56 s; Day 2: 57.01 \pm 7.14 s; Day 3: 42.89 \pm 5.74 s; Day 4: 35.84 \pm 5.45 s; Day 5: 28.94 \pm 4.44 s; $p = .003$ vs. AD + AAV_{EGFP}; Figure 5a) compared to those in AD group, whereas AAV_{shTRPV1} (AD + AAV_{shTRPV1}, $n = 24$) treatment displayed no difference with the AD group (Day 1: 89.23 \pm 4.09 s; Day 2: 70.82 \pm 5.99 s; Day 3: 68.52 \pm 6.58 s; Day 4: 54.49 \pm 5.77 s; Day 5: 59.29 \pm 7.23 s; $p = .964$ vs. AD + AAV_{EGFP}; Figure 5a). Twenty-four hours after the last training trial, a probe

test with the platform removed was performed to examine long-term spatial memory retrieval. The results revealed that spatial memory retrieval dramatically impaired in AD mice since the number of entries into the platform zone was reduced (WT: 4.13 \pm 0.71; AD + AAV_{EGFP}: 2.00 \pm 0.46, $p = .008$ vs. WT; Figure 5b). AAV_{TRPV1} treatment significantly increased the number of entries into the platform zone (AD + AAV_{TRPV1}: 3.68 \pm 0.54, $p = .571$ vs. WT, $p = .028$ vs. AD + AAV_{EGFP}; Figure 5b), whereas AAV_{shTRPV1} treatment displayed no difference compared with the AD group (AD + AAV_{shTRPV1}: 2.58 \pm 0.39, $p = .040$ vs. WT, $p = .415$ vs. AD + AAV_{EGFP}; Figure 5b).

To further evaluate the effect of TRPV1 on amelioration of learning and memory in AD model mice, we next performed another hippocampus-dependent learning and memory task, the Barnes maze test. During spatial learning period, the escape latency for finding the escape box in APP23/PS45 mice (AD + AAV_{EGFP}, $n = 8$) was much longer than those in WT mice (WT, $n = 9$) (Day 1: 85.95 \pm 15.50 s for

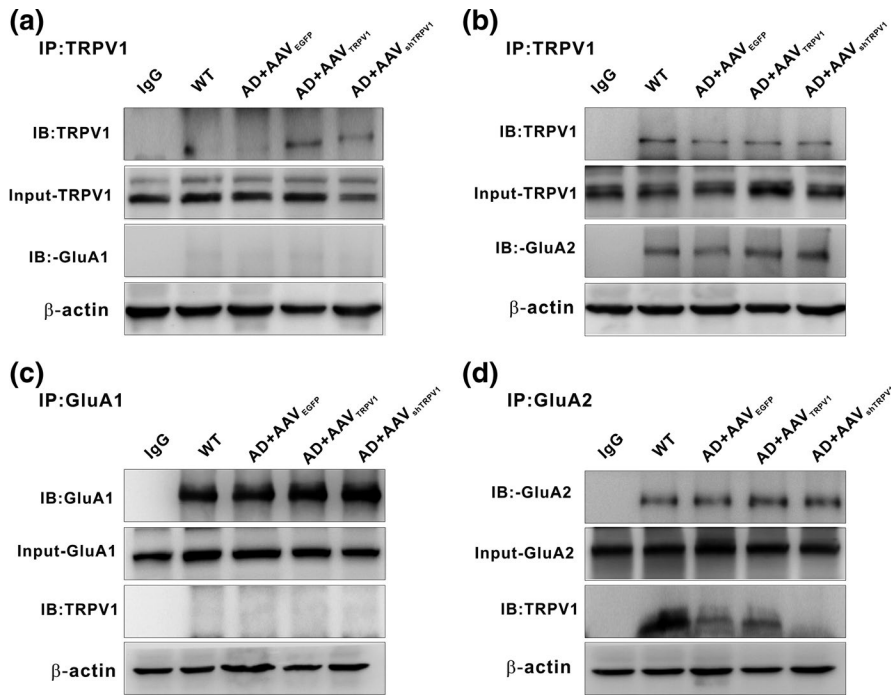


FIGURE 4 TRPV1 interacts with GluA2 subunit of AMPAR. (a and b) Immunoprecipitation (IP) of hippocampal samples from WT and APP23/PS45 mice after extraction in lysis buffer with antibodies to TRPV1 or negative control antibodies with the indicated antibodies to the TRPV1, GluA1 (a), and GluA2 (b). (c and d) IP of hippocampal samples from WT and APP23/PS45 mice after extraction in lysis buffer with antibodies to GluA1, GluA2, or IgG and immunoblot analysis with the indicated antibodies to the TRPV1, GluA1 (c), and GluA2 (d)

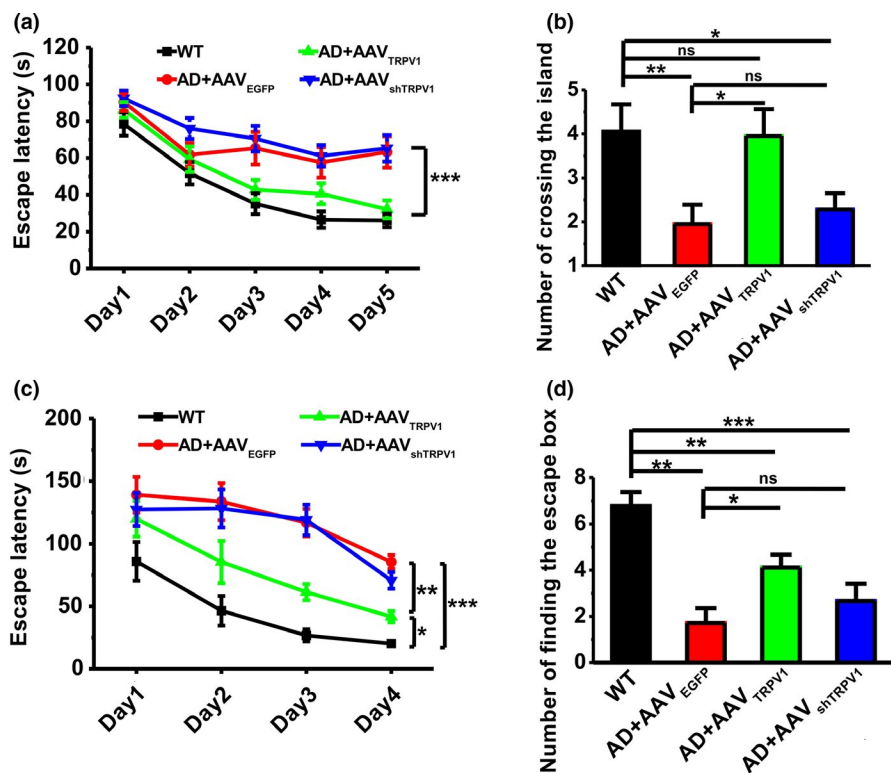
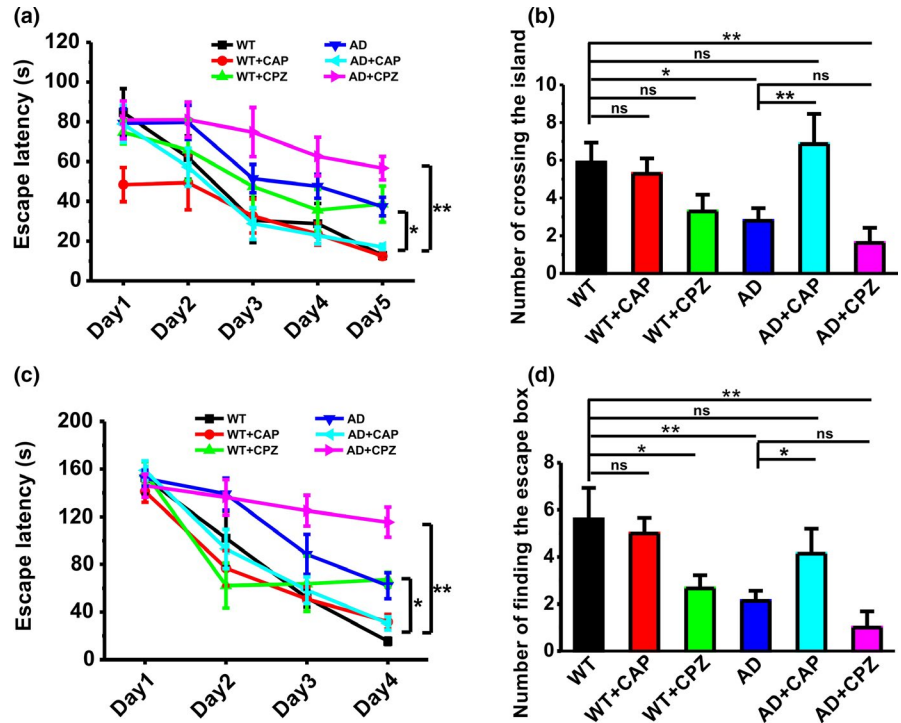


FIGURE 5 Genetic upregulation of TRPV1 rescues learning and memory deficits in APP23/PS45 mice. (a) The escape latency to the hidden platform during spatial learning in the Morris water maze paradigm ($n = 16-24$ in each group). Repeated measures ANOVA: $F_{(3,74)} = 9.748$, $p < .001$. (b) The number of entries into the platform zone. One-way ANOVA: $F_{(3,74)} = 3.281$, $p = .026$. (c) The latency to the escape box during spatial learning in the Barnes maze paradigm ($n = 8-9$ in each group). Repeated measures ANOVA: $F_{(3,41)} = 20.139$, $p < .001$. (d) The occurrence of head dips to the escape hole during memory retrieval. One-way ANOVA: $F_{(3,41)} = 10.793$, $p < .001$. Data are expressed as mean \pm SEM, * $p < .05$, ** $p < .01$, *** $p < .001$

WT, 139.07 ± 14.27 s for AD + AAV_{EGFP}; Day 2: 46.45 ± 11.88 s for WT, 133.75 ± 14.78 s for AD + AAV_{EGFP}; Day 3: 26.72 ± 4.87 s for WT, 116.93 ± 10.99 s for AD + AAV_{EGFP}; Day 4: 20.12 ± 1.34 s for WT, 85.48 ± 5.59 s for AD + AAV_{EGFP}; $p < .001$ vs. WT; Figure 5c). AAV_{TRPV1} (AD + AAV_{TRPV1}, $n = 9$) treatment significantly shortened escape latency for searching for the escape box (Day 1: 119.95 ± 14.28 s; Day 2: 5.37 ± 16.93 s; Day 3: 61.31 ± 6.42 s; Day 4: 41.70 ± 4.58 s; $p = .001$ vs. AD + AAV_{EGFP}; Figure 5c), whereas AAV_{shTRPV1} treatment

(AD + AAV_{shTRPV1}, $n = 9$) displayed no difference compared with the AD group (Day 1: 127.42 ± 13.16 s; Day 2: 128.24 ± 15.16 s; Day 3: 119.11 ± 12.22 s; Day 4: 70.66 ± 6.70 s; $p = .499$ vs. AD + AAV_{EGFP}; Figure 5c). Twenty-four hours after the last training trial, a long-term spatial memory retrieval test was performed with the escape box blocked. The results showed that memory retrieval was impaired in AD model mice since the number of finding the escape box was significantly decreased compared to WT control (WT: 6.78 ± 0.60 ;

FIGURE 6 Capsaicin rescues learning and memory deficits in APP23/PS45 mice. (a) The escape latency to the hidden platform during spatial learning in the Morris water maze paradigm ($n = 7-10$ in each group). Repeated measures ANOVA: $F_{(5,42)} = 6.274$, $p < .001$. (b) The number of entries into the platform zone. One-way ANOVA: $F_{(5,42)} = 4.276$, $p = .003$. (c) The latency to the escape box during spatial learning in the Barnes maze paradigm ($n = 5-8$ in each group). Repeated measures ANOVA: $F_{(5,37)} = 8.805$, $p < .001$. (d) The occurrence of head dips to the escape hole during memory retrieval. One-way ANOVA: $F_{(5,37)} = 5.024$, $p = .001$. Data are expressed as mean \pm SEM, * $p < .05$, ** $p < .01$



AD + AAV_{EGFP}: 1.71 ± 0.64 ; $p < .001$ vs. WT; Figure 5d). AAV_{TRPV1} treatment increased the number of finding the escape box (AD + AAV_{TRPV1}: 4.11 ± 0.56 , $p = .006$ vs. WT, $p = .030$ vs. AD + AAV_{EGFP}; Figure 5d), whereas AAV_{shTRPV1} treatment displayed no difference compared to AD group (AD + AAV_{shTRPV1}: 2.67 ± 0.75 , $p < .001$ vs. WT, $p = .477$ vs. AD + AAV_{EGFP}; Figure 5d). Besides learning and memory deficits, patients with AD are often accompanied by depression, and laboratory research has shown that TRPV1 activation may affect anxiogenic responses and depression-related behaviors (Abdelhamid, Kovacs, Nunez, & Larson, 2014; Kasckow, Mulchahey, & Geraciotti, 2004). We here further found that TRPV1 upregulation by AAV_{TRPV1} could significantly ameliorate anxiety- and depression-like behaviors in APP23/PS45 mice during the elevated plus maze (Figure 2a and b), three-chambered social interaction (Figure 2c), and force swimming tests (Figure 2d). Collectively, these results indicate that genetic upregulation of TRPV1 by AAV microinjection succeeds in rescuing the decline of cognitive and emotional functions in AD model mice.

2.5 | Pharmacological activation of TRPV1 rescues memory decline in APP23/PS45 mice

As genetic upregulation of TRPV1 is difficult to be used in the clinical treatment, we next wanted to determine whether pharmacological activation of TRPV1 by its agonist capsaicin (CAP, 1 mg/kg, i.p.) is able to ameliorate the spatial learning and memory deficits in AD model mice. The Morris water maze and Barnes maze tests were used to measure the spatial learning and memory in mice treated with CAP or TRPV1 antagonist capsazepine (CPZ, 1 mg/kg, i.p.). The results showed that CAP treatment (WT + CAP: $n = 7$; 48.42 ± 8.62 s on Day 1, 49.39 ± 13.65 s on Day 2, 32.61 ± 8.63 s on Day 3, 23.54 ± 5.58 s

on Day 4, 12.46 ± 1.42 s on Day 5; $p = .191$ vs. WT; Figure 6a) had no effect on spatial learning during the Morris water maze test in WT mice (WT: $n = 8$; 84.67 ± 12.05 s on Day 1, 62.01 ± 10.98 s on Day 2, 30.58 ± 11.32 s on Day 3, 28.78 ± 10.17 s on Day 4, 12.74 ± 1.50 s on Day 5; Figure 6a), as reflected by taking similar time to find the hidden platform. However, the escape latency for searching for the hidden platform in APP23/PS45 mice treated with CAP was significantly shortened (AD + CAP: $n = 7$; 78.89 ± 9.34 s on Day 1, 57.20 ± 9.58 s on Day 2, 28.85 ± 7.98 s on Day 3, 22.80 ± 4.28 s on Day 4, 17.03 ± 1.39 s on Day 5; $p = .020$ vs. AD; Figure 6a), compared to vehicle treatment (AD: $n = 10$; 79.24 ± 7.22 s on Day 1, 79.62 ± 8.59 s on Day 2, 51.43 ± 7.09 s on Day 3, 47.58 ± 6.05 s on Day 4, 37.34 ± 4.66 s on Day 5; $p = .040$ vs. WT; Figure 6a). Notably, TRPV1 antagonist capsazepine (CPZ, 1 mg/kg, i.p.) administration did not affect the escape latency for searching for the hidden platform in both WT (WT + CPZ: $n = 7$; 74.71 ± 5.84 s on Day 1, 65.80 ± 15.18 s on Day 2, 47.48 ± 11.07 s on Day 3, 35.58 ± 10.42 s on Day 4, 38.67 ± 9.09 s on Day 5; $p = .275$ vs. WT; Figure 6a) and APP23/PS45 mice (AD + CPZ: $n = 8$; 80.87 ± 9.56 s on Day 1, 81.06 ± 8.89 s on Day 2, 74.81 ± 12.38 s on Day 3, 62.55 ± 9.71 s on Day 4, 56.66 ± 5.91 s on Day 5; $p = .100$ vs. AD; Figure 6a), compared to vehicle treatment. The results from long-term spatial memory retrieval test revealed that treatment with CAP (AD + CAP: 6.86 ± 1.61 , $p = .490$ vs. WT, $p = .004$ vs. AD; Figure 6b), but not CPZ (AD + CPZ: 1.63 ± 0.80 s, $p = .003$ vs. WT, $p = .368$ vs. AD; Figure 6b), reversed the memory decline in APP23/PS45 mice since the number of entries into the platform zone was dramatically increased, compared to vehicle treatment.

Next, we also evaluate the effects of CAP on learning and memory in APP23/PS45 mice in the paradigm of Barnes maze performance. The escape latency for searching for the escape box in APP23/PS45 mice (AD: $n = 8$; 152.21 ± 6.66 s on Day 1, 139.01 ± 13.53 s on Day 2,

88.49 ± 16.78 s on Day 3, 62.06 ± 10.95 s on Day 4; $p = .015$ vs. WT; Figure 6c) was much longer than those in WT (WT: $n = 5$; 152.81 ± 13.99 s on Day 1, 102.02 ± 22.79 s on Day 2, 51.86 ± 7.60 s on Day 3, 15.47 ± 2.69 s on Day 4; Figure 6c). CAP treatment (AD + CAP: $n = 7$; 158.75 ± 8.24 s on Day 1, 93.00 ± 16.43 s on Day 2, 58.49 ± 11.06 s on Day 3, 30.53 ± 5.54 s on Day 4; $p = .023$ vs. AD; Figure 6c) significantly shortened escape latency for searching for the escape box, whereas CPZ did not affect the escape latency (AD + CPZ: $n = 7$; 146.03 ± 9.65 s on Day 1, 136.32 ± 14.92 s on Day 2, 125.04 ± 12.96 s on Day 3, 115.42 ± 12.61 s on Day 4; $p = .065$ vs. AD; Figure 6c). The results from long-term spatial memory retrieval test showed that CAP (AD + CAP: 4.14 ± 1.06, $p = .237$ vs. WT, $p = .043$ vs. AD; Figure 6d), but not CPZ (AD + CPZ: 1.00 ± 0.69, $p = .001$ vs. WT, $p = .301$ vs. AD; Figure 6d), reversed the memory deficits in APP23/PS45 mice, as reflected by much more times to finding the escape box. Taken together, these findings indicate that pharmacological activation of TRPV1 by CAP significantly reverses the memory decline in AD model mice.

3 | DISCUSSION

In the present study, we find that TRPV1 expression is significantly reduced in the brains of APP23/PS45 transgenic model mice of AD. We also report that upregulation of TRPV1 alleviates AD-related neuropathologies and inhibits AMPAR endocytosis via interacting with GluA2 subunit, which may subsequently contribute to the amelioration of cognitive function and synaptic plasticity. Meanwhile, TRPV1 activation by CAP could also improve the learning and memory in APP23/PS45 double transgenic mice. Collectively, the current study demonstrates the protective effect of TRPV1 on AD pathogenesis, suggesting that it may serve as a potential therapeutic molecule for AD.

Progressive cognitive decline is the main clinical symptom in AD, and synaptic plasticity is generally accepted as a critical phenomenon used by the brain for adapting or learning from experiences in our environment (Bliss & Collingridge, 1993; Collingridge et al., 2004; Malenka & Nicoll, 1999). It has recently been demonstrated that TRPV1 channels are widely expressed in the central nervous system and participate in long-term synaptic plasticity in the CA1 region (Hurtado-Zavala et al., 2017; Li et al., 2008; Marsch et al., 2007; Mezey et al., 2000; Toth et al., 2005). Thus, regulation of TRPV1 may alleviate synaptic and cognitive impairments during AD development. Indeed, our recent study has demonstrated that TRPV1 activation by CAP could improve the synaptic and cognitive functions in A β -induced mouse model of AD (Chen et al., 2017). Jiang and colleagues have also reported that activation of TRPV1 can mitigate stress-induced AD-like neuropathological alterations and cognitive impairment in rats (Jiang et al., 2013). Accordingly, in the present study, we found that upregulation of TRPV1 by AAV microinjection succeeded in ameliorating the synaptic and cognitive functions in APP23/PS45 transgenic mouse model of AD. We also reported that pharmacological activation of TRPV1 by its agonist CAP could rescue the deficits of spatial learning and memory in the APP23/PS45 mice, indicating that activation of TRPV1 may serve as a potential strategy for AD treatment.

To date, despite the fact that all of the clinical trials for AD focused on A β have failed, accumulating evidence from laboratories and clinics worldwide supports the view that an imbalance between production and clearance of A β and related A β peptides is a very early, often initiating factor during the progression of AD (Beyreuther & Masters, 1991; Hardy & Higgins, 1992; Selkoe, 1991). Therefore, A β has been generally recognized as the culprit of AD (Wilcock & Griffin, 2013), which was generated from proteolytic cleavages of APP by the β - and γ -secretases (Querfurth & LaFerla, 2010), and reducing the amount of A β might be a potential therapeutic strategy for AD. TRPV1 activation causes Ca²⁺ influx, and dysregulation of Ca²⁺ is involved in the pathogenesis of AD. For instance, the levels of calcium activity are increased in AD patients (Johnson et al., 1997) and elevated Ca²⁺ induce BACE1 expression and consequently result in an increase in A β production (Cho, Jin, Youn, Huh, & Mook-Jung, 2008; Mata, 2018) and cell death (Pierrot, Ghisdal, Caumont, & Octave, 2004). However, contradictory results have shown that familial AD-linked PS1 or PS2 mutation attenuates calcium entry and thus increasing A β production (Fedeli, Filadi, Rossi, Mammucari, & Pizzo, 2019; Yoo et al., 2000), whereas constitutive activation of Ca²⁺ entry reduces A β secretion (Zeiger et al., 2013). Thus, genetic or pharmacological activation of TRPV1 may increase Ca²⁺ influx, reduce APP processing, and consequently improve synaptic plasticity and memory in APP23/PS45 model mice of AD.

It has been well documented that A β accumulation could dramatically interfere with synaptic transmission, leading to impairment of LTP (Nalbantoglu et al., 1997; Shankar et al., 2008), and the GluA2-dependent AMPAR endocytosis contributes to the decay of LTP, thereby impairing learning and memory (Dong et al., 2015). However, the mechanisms by which induced AMPAR endocytosis are still unclear. Here, we reported that AMPAR endocytosis was increased in APP23/PS45 transgenic mice, and upregulation of TRPV1 by AAV microinjection significantly reduced AMPAR endocytosis. Importantly, TRPV1 was able to interact with GluA2, but not GluA1, and their interactions were reduced in APP23/PS45 transgenic mice. Upregulation of TRPV1 may prolong activation of AMPAR in the hippocampus due to enhanced Ca²⁺ influx following TRPV1 activation, and thereby inhibiting GluA2-dependent AMPAR endocytosis. Notably, how TRPV1 interacts with GluA2 remains to be further detected.

In summary, our study demonstrates that genetic or pharmacological activation of TRPV1 not only improves hippocampal LTP and memory but also reduces neuritic plaques in mouse model of AD, suggesting a potential therapeutic role of TRPV1 for learning and memory deficits associated with both patients with AD and aged populations.

4 | EXPERIMENTAL PROCEDURES

4.1 | Animals

APP23/PS45 transgenic mice were maintained at Children's Hospital of Chongqing Medical University Animal Care Centre. Mice were housed under 12-hr light and 12-hr dark cycle (lights

on from 7:00 a.m. to 7:00 p.m.) with free access to food and water in a temperature and humidity controlled SPF room. The genotype of the mice was confirmed by PCR using DNA from tail tissues. All animal experiments were conducted in accordance with the Chongqing Science and Technology Commission guidelines and approved by the Chongqing Medical University Animal Care Committee.

4.2 | Drugs and treatment

TRPV1 agonist capsaicin (CAP) and antagonist capsazepine (CPZ) were purchased from Sigma-Aldrich, which were dissolved in a 1:1:8 mixture of Tween 80: ethanol: saline. Mice received drug injection daily from the age of 1.5 months to the end of the behavioral test.

4.3 | Adeno-associated virus and microinjection

To overexpress or knockdown TRPV1 *in vivo*, adeno-associated virus-mediated TRPV1 (AAV_{TRPV1}) or TRPV1 small hairpin RNA (AAV_{shTRPV1}) was constructed by OBiO Technology (Shanghai, China). Titers were 3×10^{12} TU/ml. Mice were anesthetized with sodium pentobarbital (60 mg/kg, *i.p.*), and the core temperature was maintained at $36.5 \pm 0.5^\circ\text{C}$. Atropine (0.4 mg/kg, *i.p.*) was also given to help relieve respiratory congestion. Scalp skin was shaved with clippers and disinfected using iodine before mice were mounted on a stereotaxic instrument. After opening the scalp skin and exposing the skull, 1 μl of AAV_{TRPV1} or AAV_{shTRPV1} was microinjected into each hippocampal CA1 area by drilled hole (-2.3 mm and -2.5 mm posterior, ± 2.0 mm lateral and 2.5 mm ventral relative to bregma). Animals received AAV microinjections at the age of 1.5 months and performed behavioral test at the age of 3 months.

4.4 | Morris water maze test

The Morris water maze consists of a circular stainless steel pool (150 cm in diameter) filled with opaque white paint as previously described (Dong et al., 2015; Du et al., 2019). The pool was surrounded by light blue curtains, and 3 distal visual cues were fixed to the curtains. A CCD camera was suspended above the pool center to record the animal's swimming path, and video output was digitized by an ANY-maze tracking system (Stoelting). Twenty-four hours before spatial training, the animals were allowed to adapt to the maze for a 120-s free swim. The animals were then trained in the spatial learning task for 4 trials per day for 5 consecutive days. In each trial, mice were placed into water from 4 starting positions (NE, NW, SW, and SE), facing to the pool wall. They were then required to swim to find the hidden platform (7.5 cm in diameter), which was submerged 1 cm below the opaque water surface in a fixed position in the SW

quadrant. During each trial, mice were allowed to swim until they found the hidden platform where they remained for 20 s before being returned to home cage. Mice that failed to find the hidden platform in 120 s were guided to the platform where they remained for 20 s. Twenty-four hours after the final training trial, a probe test was conducted. Mice were returned to the pool from a novel drop point with the hidden platform absent for 120 s, and their swim path was recorded.

4.5 | Barnes maze test

The apparatus consists of a white circular platform 0.75 m in diameter, with 18 holes (5 cm in diameter) placed at the edges, and with an escape box located underneath one of these holes as previously described (Yu et al., 2018). A CCD camera suspended above the maze center records the latency and count of errors of finding the escape box, and video outputs are digitized by an ANY-maze video tracking system (Stoelting). Twenty-four hours before spatial training, the animals were allowed to adapt to the maze for 3 min. The animals were then trained in spatial learning task for 4 trials per day for 4 days, with an inter-trial interval of 15 min. In each trial, the animal was placed in the center of the maze, and the time travelled to get to the escape box was measured. If the animal found and entered into the box within 3 min, the animal was returned to its home cage; if the animal failed to find the escape box, or if it found the box but did not enter into the box within 3 min, it would be gently guided to the box and held there for 60 s before being returned to the home cage. Twenty-four hours after the final training trial, mice were returned to the maze and a 3-min probe test was performed with the escape box blocked.

4.6 | Electrophysiology *in vitro*

Mice (4 months old) were deeply anesthetized with urethane (1.5 g/kg, *i.p.*) and transcardially perfused with artificial cerebral spinal fluid (ACSF) (in mM: NaCl 124, KCl 2.8, $\text{NaH}_2\text{PO}_4 \cdot \text{H}_2\text{O}$ 1.25, CaCl_2 2.0, MgSO_4 1.2, Na-vitamin C 0.4, NaHCO_3 26, Na-lactate 2.0, Na-pyruvate 2.0 and D-glucose 10.0, pH = 7.4) prior to decapitation as described previously (Du et al., 2019; Huang et al., 2017). Then, hippocampal slices were coronally sectioned (400 μm) with a vibratome (VT1200S, Leica Microsystems, Bannockburn, IL) with 95% O_2 and 5% CO_2 , and then were incubated in ACSF for 2 hr at 35°C . A bipolar stimulating electrode was placed at the Schaffer collaterals of dorsal hippocampus CA3 pyramidal neurons, and a recording pipette filled with ACSF was placed at the ipsilateral striatum radiatum of the hippocampal CA1 area. An input-output curve was measured at different current stimulation from 0.05 to 0.4 mA, and test EPSPs were evoked at a frequency of 0.05 Hz and at a stimulus intensity adjusted to around 50% of the maximal response size. After a 30-min stable baseline, theta burst stimulation (TBS) was given to induce LTP. TBS consisted of 2 trains of stimuli (at 20 s interval), with each train composed

of 5 bursts (4 pulses at 100 Hz in each burst) at an inter-burst interval of 200 ms. Data acquisition was performed with the PatchMaster v2.73 software (HEKA Elektronik, Lambrecht/Pfalz, Germany).

4.7 | Immunohistochemistry staining

Mice were euthanized with urethane (3 g/kg, i.p., Sigma) after behavioral testing, and one-half of the brain was immediately frozen for protein or RNA extraction. The other half of the brain was postfixed in freshly 4% paraformaldehyde (PFA) in 0.1 M phosphate-buffered saline (PBS, pH 7.4) for 24 hr. Then, the brain was dehydrated with 30% sucrose until it sank to the bottom and serially cut into 30 μ m thick coronal sections using Leica Instrument. The sections were incubated with 3% H₂O₂ to remove residual peroxidase activity for 30 min. Then, slices were blocked with 10% BSA and incubated with mouse monoclonal 4G8 antibody (1:500) overnight at 4°C. Sections were mounted onto slides, and plaques were visualized by the ABC and DAB method and counted by microscopy at \times 40 magnification. The mean plaque count per slice was recorded for each mouse as described previously (Dong et al., 2015; Du et al., 2019).

4.8 | Western blot assay

After behavioral testing, the hippocampus and cerebral cortex were dissected and weighed immediately and then homogenized in homogeneous buffer in a mortar and pestle. The homogenates were centrifuged (4°C, 12,000 g, 15 min) to collect the supernatants. The protein concentration was measured with a BCA protein assay reagent (Thermo Fisher Scientific, Waltham, MA, USA) according to the manufacturer's instruction. Uniform amount of each protein samples (30 μ g) was boiled with 5 \times loading buffer at 95°C for 10 min. The samples were then separated on 10% SDS-PAGE and transferred onto an immobilon-PTM polyvinylidene fluoride (PVDF) membrane. To block nonspecific background, the membranes were incubated with 5% nonfat milk in Tris-buffered saline containing 0.1% Tween-20 (TBST) at 37°C for 1 hr. The target proteins were immunoblotted with primary antibody overnight at 4°C to APP (obtained from Professor Weihong Song), BACE1 (1:2000; CST, USA), PS1 (1:3,000; Abcam, USA), TRPV1 (1:200; Millipore, USA), GluA1 (1:500; Abcam, USA), and GluA2 (1:1,000; Abcam, USA). After incubation with goat anti-rabbit IgG (1:3,000; Abcam, USA) at 37°C for 1 hr, the protein was visualized in the Bio-Rad Imager using ECL Western blotting substrate (Pierce). β -actin was the internal reference. The band intensity of each protein was quantified by the Bio-Rad Quantity One software as described previously (Dong et al., 2015; Du et al., 2019).

4.9 | Co-immunoprecipitation

Cerebral hippocampus was homogenized in ice-cold Co-IP lysis buffer and proteinase inhibitor mixture. After clearing debris by centrifuge at 12,000 g at 4°C, protein concentration in the extracts was

determined by BCA assay. The hippocampal samples (500 μ g) were incubated with nonspecific IgG or polyclonal rabbit anti-Glu A1 or anti-Glu A2 overnight at 4°C, followed by the addition of 40 μ l of protein G for 3 hr at 4°C. The precipitate was washed four times with lysis buffer and denatured with SDS sample buffer and separated by 10% SDS-PAGE.

4.10 | Statistical analysis

All data are expressed as mean \pm SEM. ANOVA or two-tailed Student's *t* tests were used to analyze the data by where appropriate. The significance level was set at $p < 0.05$.

ACKNOWLEDGMENTS

This work was supported by grants from the National Natural Science Foundation of China (No. 81622015, 91749116, and 81571042), the Science and Technology Research Program of Chongqing Municipal Education Commission (No. KJZD-K201900403), Innovation Research Group at Institutions of Higher Education in Chongqing (No. CXQTP19019019034), and Natural Science Foundation of Chongqing (No. cstc2019jcyj-bshX0016).

CONFLICT OF INTEREST

The authors have declared that no conflict of interest exists.

AUTHOR CONTRIBUTIONS

YD, MF, and XT performed behavioral and biochemical experiments. ZH and JL performed electrophysiological experiments. YD, JL, and YP analyzed the data. ZD designed the research study and contributed essential reagents or tools. YD and ZD wrote the manuscript. WS and YTW provided helpful discussion.

DATA AVAILABILITY STATEMENT

The data that support the findings of this study are available from the corresponding author upon reasonable request.

ORCID

Zhifang Dong  <https://orcid.org/0000-0002-3411-7923>

REFERENCES

- Abdelhamid, R. E., Kovacs, K. J., Nunez, M. G., & Larson, A. A. (2014). Depressive behavior in the forced swim test can be induced by TRPV1 receptor activity and is dependent on NMDA receptors. *Pharmacological Research*, *79*, 21–27. <https://doi.org/10.1016/j.phrs.2013.10.006>
- Beyreuther, K., & Masters, C. L. (1991). Amyloid precursor protein (APP) and beta A4 amyloid in the etiology of Alzheimer's disease: Precursor-product relationships in the derangement of neuronal function. *Brain Pathology*, *1*(4), 241–251.
- Bliss, T. V., & Collingridge, G. L. (1993). A synaptic model of memory: Long-term potentiation in the hippocampus. *Nature*, *361*(6407), 31–39. <https://doi.org/10.1038/361031a0>
- Chen, L., Huang, Z., Du, Y., Fu, M., Han, H., Wang, Y., & Dong, Z. (2017). Capsaicin attenuates amyloid-beta-induced synapse loss and

- cognitive impairments in mice. *Journal of Alzheimer's Disease*, 59(2), 683–694. <https://doi.org/10.3233/JAD-170337>
- Cho, H. J., Jin, S. M., Youn, H. D., Huh, K., & Mook-Jung, I. (2008). Disrupted intracellular calcium regulates BACE1 gene expression via nuclear factor of activated T cells 1 (NFAT 1) signaling. *Aging Cell*, 7(2), 137–147. <https://doi.org/10.1111/j.1474-9726.2007.00360.x>
- Collingridge, G. L., Isaac, J. T., & Wang, Y. T. (2004). Receptor trafficking and synaptic plasticity. *Nature Reviews Neuroscience*, 5(12), 952–962. <https://doi.org/10.1038/nrn1556>
- Davis, J. N. 2nd, & Chisholm, J. C. (1999). Alois Alzheimer and the amyloid debate. *Nature*, 400(6747), 810. <https://doi.org/10.1038/23571>
- Dong, Z., Han, H., Li, H., Bai, Y., Wang, W., Tu, M., ... Wang, Y. T. (2015). Long-term potentiation decay and memory loss are mediated by AMPAR endocytosis. *Journal of Clinical Investigation*, 125(1), 234–247. <https://doi.org/10.1172/JCI77888>
- Du, Y., Du, Y., Zhang, Y., Huang, Z., Fu, M., Li, J., ... Dong, Z. (2019). MKP-1 reduces Aβ generation and alleviates cognitive impairments in Alzheimer's disease models. *Signal Transduction and Targeted Therapy*, 4, 58. <https://doi.org/10.1038/s41392-019-0091-4>
- Fedeli, C., Filadi, R., Rossi, A., Mammucari, C., & Pizzo, P. (2019). PSEN2 (presenilin 2) mutants linked to familial Alzheimer disease impair autophagy by altering Ca(2+) homeostasis. *Autophagy*, 15(12), 2044–2062. <https://doi.org/10.1080/15548627.2019.1596489>
- Fu, M., Xie, Z., & Zuo, H. (2009). TRPV1: A potential target for anti-epileptogenesis. *Medical Hypotheses*, 73(1), 100–102. <https://doi.org/10.1016/j.mehy.2009.01.005>
- Goedert, M., Jakes, R., Spillantini, M. G., Hasegawa, M., Smith, M. J., & Crowther, R. A. (1996). Assembly of microtubule-associated protein tau into Alzheimer-like filaments induced by sulphated glycosaminoglycans. *Nature*, 383(6600), 550–553. <https://doi.org/10.1038/383550a0>
- Hardy, J. A., & Higgins, G. A. (1992). Alzheimer's disease: The amyloid cascade hypothesis. *Science*, 256(5054), 184–185. <https://doi.org/10.1126/science.1566067>
- Hsieh, H., Boehm, J., Sato, C., Iwatsubo, T., Tomita, T., Sisodia, S., & Malinow, R. (2006). AMPAR removal underlies Aβ-induced synaptic depression and dendritic spine loss. *Neuron*, 52(5), 831–843. <https://doi.org/10.1016/j.neuron.2006.10.035>
- Huang, Z., Tan, T., Du, Y., Chen, L., Fu, M., Yu, Y., ... Dong, Z. (2017). Low-frequency repetitive transcranial magnetic stimulation ameliorates cognitive function and synaptic plasticity in APP23/PS45 mouse model of Alzheimer's Disease. *Frontiers in Aging Neuroscience*, 9, 292. <https://doi.org/10.3389/fnagi.2017.00292>
- Hurtado-Zavala, J. I., Ramachandran, B., Ahmed, S., Halder, R., Bolleyer, C., Awasthi, A., ... Dean, C. (2017). TRPV1 regulates excitatory innervation of OLM neurons in the hippocampus. *Nature Communications*, 8, 15878. <https://doi.org/10.1038/ncomms15878>
- Jiang, X., Jia, L.-W., Li, X.-H., Cheng, X.-S., Xie, J.-Z., Ma, Z.-W., ... Zhou, X.-W. (2013). Capsaicin ameliorates stress-induced Alzheimer's disease-like pathological and cognitive impairments in rats. *Journal of Alzheimer's Disease*, 35(1), 91–105. <https://doi.org/10.3233/JAD-121837>
- Johnson, G. V., Cox, T. M., Lockhart, J. P., Zinnerman, M. D., Miller, M. L., & Powers, R. E. (1997). Transglutaminase activity is increased in Alzheimer's disease brain. *Brain Research*, 751(2), 323–329. [https://doi.org/10.1016/S0006-8993\(96\)01431-X](https://doi.org/10.1016/S0006-8993(96)01431-X)
- Kamenetz, F., Tomita, T., Hsieh, H., Seabrook, G., Borchelt, D., Iwatsubo, T., ... Malinow, R. (2003). APP processing and synaptic function. *Neuron*, 37(6), 925–937. [https://doi.org/10.1016/S0896-6273\(03\)00124-7](https://doi.org/10.1016/S0896-6273(03)00124-7)
- Kasckow, J. W., Mulchahey, J. J., & Geraciotti, T. D. Jr (2004). Effects of the vanilloid agonist olvanil and antagonist capsazepine on rat behaviors. *Progress in Neuro-Psychopharmacology and Biological Psychiatry*, 28(2), 291–295. <https://doi.org/10.1016/j.pnpbp.2003.10.007>
- Li, H. B., Mao, R. R., Zhang, J. C., Yang, Y., Cao, J., & Xu, L. (2008). Antistress effect of TRPV1 channel on synaptic plasticity and spatial memory. *Biological Psychiatry*, 64(4), 286–292. <https://doi.org/10.1016/j.biopsych.2008.02.020>
- Malenka, R. C., & Nicoll, R. A. (1999). Long-term potentiation—a decade of progress? *Science*, 285(5435), 1870–1874.
- Marsch, R., Foeller, E., Rammes, G., Bunck, M., Kossel, M., Holsboer, F., ... Wotjak, C. T. (2007). Reduced anxiety, conditioned fear, and hippocampal long-term potentiation in transient receptor potential vanilloid type 1 receptor-deficient mice. *Journal of Neuroscience*, 27(4), 832–839. <https://doi.org/10.1523/JNEUROSCI.3303-06.2007>
- Mata, A. M. (2018). Functional interplay between plasma membrane Ca(2+)-ATPase, amyloid beta-peptide and tau. *Neuroscience Letters*, 663, 55–59. <https://doi.org/10.1016/j.neulet.2017.08.004>
- Mezey, E., Toth, Z. E., Cortright, D. N., Arzubi, M. K., Krause, J. E., Elde, R., ... Szallasi, A. (2000). Distribution of mRNA for vanilloid receptor subtype 1 (VR1), and VR1-like immunoreactivity, in the central nervous system of the rat and human. *Proceedings of the National Academy of Sciences*, 97(7), 3655–3660. <https://doi.org/10.1073/pnas.060496197>
- Nalbantoglu, J., Tirado-Santiago, G., Lahsaini, A., Poirier, J., Goncalves, O., Verge, G., ... Shapiro, M. L. (1997). Impaired learning and LTP in mice expressing the carboxy terminus of the Alzheimer amyloid precursor protein. *Nature*, 387(6632), 500–505. <https://doi.org/10.1038/387500a0>
- Peters, J. H., McDougall, S. J., Fawley, J. A., Smith, S. M., & Andresen, M. C. (2010). Primary afferent activation of thermosensitive TRPV1 triggers asynchronous glutamate release at central neurons. *Neuron*, 65(5), 657–669. <https://doi.org/10.1016/j.neuron.2010.02.017>
- Pierrot, N., Ghisdal, P., Caumont, A. S., & Octave, J. N. (2004). Intraneuronal amyloid-beta1-42 production triggered by sustained increase of cytosolic calcium concentration induces neuronal death. *Journal of Neurochemistry*, 88(5), 1140–1150. <https://doi.org/10.1046/j.1471-4159.2003.02227.x>
- Querfurth, H. W., & LaFerla, F. M. (2010). Alzheimer's disease. *New England Journal of Medicine*, 362(4), 329–344. <https://doi.org/10.1056/NEJMra0909142>
- Roselli, F., Tirard, M., Lu, J., Hutzler, P., Lamberti, P., Livrea, P., ... Almeida, O. F. (2005). Soluble beta-amyloid1-40 induces NMDA-dependent degradation of postsynaptic density-95 at glutamatergic synapses. *Journal of Neuroscience*, 25(48), 11061–11070. <https://doi.org/10.1523/JNEUROSCI.3034-05.2005>
- Sawamura, S., Shirakawa, H., Nakagawa, T., Mori, Y., & Kaneko, S. (2017). TRP Channels in the Brain: What Are They There For? In T. L. R. Emir (Ed.), *Neurobiology of TRP Channels* (pp. 295–322). Boca Raton, FL: CRC Press/Taylor & Francis. <https://doi.org/10.4324/9781315152837-16>
- Selkoe, D. J. (1991). The molecular pathology of Alzheimer's disease. *Neuron*, 6(4), 487–498. [https://doi.org/10.1016/0896-6273\(91\)90052-2](https://doi.org/10.1016/0896-6273(91)90052-2)
- Shankar, G. M., Li, S., Mehta, T. H., Garcia-Munoz, A., Shepardson, N. E., Smith, I., ... Selkoe, D. J. (2008). Amyloid-beta protein dimers isolated directly from Alzheimer's brains impair synaptic plasticity and memory. *Nature Medicine*, 14(8), 837–842. <https://doi.org/10.1038/nm1782>
- Snyder, E. M., Nong, Y., Almeida, C. G., Paul, S., Moran, T., Choi, E. Y., ... Greengard, P. (2005). Regulation of NMDA receptor trafficking by amyloid-beta. *Nature Neuroscience*, 8(8), 1051–1058. <https://doi.org/10.1038/nn1503>
- Takahashi, N., & Mori, Y. (2011). TRP Channels as Sensors and Signal Integrators of Redox Status Changes. *Frontiers in Pharmacology*, 2, 58. <https://doi.org/10.3389/fphar.2011.00058>
- Tóth, A., Boczán, J., Kedei, N., Lizanecz, E., Bagi, Z., Papp, Z., ... Blumberg, P. M. (2005). Expression and distribution of vanilloid receptor 1 (TRPV1) in the adult rat brain. *Molecular Brain Research*, 135(1–2), 162–168. <https://doi.org/10.1016/j.molbrainres.2004.12.003>

- Wilcock, D. M., & Griffin, W. S. (2013). Down's syndrome, neuroinflammation, and Alzheimer neuropathogenesis. *Journal of Neuroinflammation*, 10, 84. <https://doi.org/10.1186/1742-2094-10-84>
- Yoo, A. S., Cheng, I., Chung, S., Grenfell, T. Z., Lee, H., Pack-Chung, E., ... Kim, T.-W. (2000). Presenilin-mediated modulation of capacitative calcium entry. *Neuron*, 27(3), 561-572. [https://doi.org/10.1016/s0896-6273\(00\)00066-0](https://doi.org/10.1016/s0896-6273(00)00066-0)
- Yu, Y., Huang, Z., Dai, C., Du, Y., Han, H., Wang, Y. T., & Dong, Z. (2018). Facilitated AMPAR endocytosis causally contributes to the maternal sleep deprivation-induced impairments of synaptic plasticity and cognition in the offspring rats. *Neuropharmacology*, 133, 155-162. <https://doi.org/10.1016/j.neuropharm.2018.01.030>
- Zeiger, W., Vetrivel, K. S., Buggia-Prevot, V., Nguyen, P. D., Wagner, S. L., Villereal, M. L., & Thinakaran, G. (2013). Ca²⁺ influx through store-operated Ca²⁺ channels reduces Alzheimer disease beta-amyloid peptide secretion. *Journal of Biological Chemistry*, 288(37), 26955-26966. <https://doi.org/10.1074/jbc.M113.473355>

SUPPORTING INFORMATION

Additional supporting information may be found online in the Supporting Information section.

How to cite this article: Du Y, Fu M, Huang Z, et al. TRPV1 activation alleviates cognitive and synaptic plasticity impairments through inhibiting AMPAR endocytosis in APP23/PS45 mouse model of Alzheimer's disease. *Aging Cell*. 2020;19:e13113. <https://doi.org/10.1111/acer.13113>